

Avalanches in Strained Amorphous Solids: Does Inertia Destroy Critical Behavior?

K. Michael Salerno, Craig E. Maloney, and Mark O. Robbins

*Department of Physics and Astronomy, Johns Hopkins University, Baltimore, Maryland 21210 USA and
Department of Civil Engineering, Carnegie Mellon University, Pittsburgh, Pennsylvania 15213*

(Dated: February 20, 2022)

Simulations are used to determine the effect of inertia on athermal shear of a two-dimensional binary Lennard-Jones glass. In the quasistatic limit, shear occurs through a series of rapid avalanches. The distribution of avalanches is analyzed using finite-size scaling with thousands to millions of particles. Inertia takes the system to a new underdamped universality class rather than driving the system away from criticality. Scaling exponents are determined for the underdamped and overdamped limits and a critical damping that separates the two regimes. Systems are in the overdamped universality class even when most vibrational modes are underdamped.

PACS numbers: 45.70.Ht, 61.43.Bn

Many slowly driven physical systems exhibit long quiescent periods punctuated by rapid avalanches [1]. Phenomena as diverse as earthquakes, Barkhausen noise in magnetic materials, dislocation cascades in single crystal microcompression and fluid interface depinning [2–8] display power law avalanche statistics in seismicity, acoustic emission, slip, stress drop or interface advance. These power laws reflect a non-equilibrium critical transition at the onset of motion.

This Letter addresses a fundamental question about the effect of inertia on such critical behavior. Power law scaling has normally been observed in overdamped systems. Studies of underdamped systems suggest that any inertia may drive the system away from the critical point [9, 10]. In sandpiles, the onset of motion appears to become a hysteretic first-order transition [11]. In the Burridge-Knopoff model, inertia leads to a growing importance of non-critical, system spanning events [12]. These conclusions about the effect of inertia seem at odds with the observation of power law scaling in earthquakes and laboratory compression tests [2, 6], where seismic waves and acoustic emission indicate that the systems are underdamped.

Here, quasistatic simulations of sheared glassy solids are performed over a full range of damping rates. The results reveal a rich phase diagram. Different universality classes describe the overdamped and underdamped limits, but both are described by critical finite-size scaling relations. The transition between the two limits occurs at a fixed damping rate that appears to have its own scaling behavior. Overdamped scaling extends to surprisingly small damping rates, where nearly all vibrational modes are underdamped. The power law describing underdamped avalanches is close to the Gutenberg-Richter law and an excess of large events is observed that is similar to observations of individual fault systems.

Since we are interested in the general question of how inertia affects critical behavior, we consider a two-dimensional binary mixture of particles that has been widely studied as a model amorphous system [13–15].

The particles may represent atoms, grains, bubbles, colloids or volume elements of a deforming fault zone. As particle size increases, temperature becomes less relevant. We focus on the athermal limit because it allows clear identification of small avalanches, and because other work indicates that temperature may also drive systems away from criticality [16, 17].

Particles interact via the Lennard-Jones (LJ) potential, $U(\mathbf{r}) = 4u_0[(a_{ij}/r)^6 - (a_{ij}/r)^{12}]$ where r is the magnitude of the vector \mathbf{r} between two particles and the species i, j are of two types, A and B. The particles have diameter $a_{AA} = 5/3 a_{BB} = a$ and $a_{AB} = 4/5 a$. The LJ energy and force are taken smoothly to zero at $r_c = 1.5a_{ij}$ using a polynomial fit starting at $1.2a_{ij}$ [18]. Both particle types have mass m and the number ratio $N_A/N_B = (1 + \sqrt{5})/4$. The depth of the inter-atomic potential u_0 sets the energy scale of particle interactions. The natural unit of time is $\tau = \sqrt{ma^2/u_0}$.

Initial states are prepared as in Ref. [18], but, as there, the protocol has little effect on steady state shear. After annealing, the system contains $N(\sim 10^3 - 10^6)$ particles in a square unit cell with edge $L = 27a$ to $875a$. The density $\rho = 1.38a^{-2}$ and the pressure is near zero. A pure shear strain is applied to the system by changing the periodic boundaries while holding area constant. The strain rate $|\dot{\epsilon}| < 10^{-6}\tau^{-1}$ between avalanches was adjusted for each L to ensure simulations were in the quasistatic limit where results depend only on strain interval and not independently on time. When an increase in kinetic energy indicated the onset of plastic deformation, $|\dot{\epsilon}|$ was reduced to zero to allow the avalanche to evolve without external perturbation. Shearing resumed after the kinetic energy dropped below 1% of the background value during shear.

In order to model the athermal limit, the kinetic energy released during avalanches must be removed by some damping mechanism. Unless noted, a viscous drag force was applied to each particle $\mathbf{F}_{drag} = -\Gamma m \mathbf{v}$ where \mathbf{v} is the non-affine velocity. As the dissipation rate Γ decreases, the dynamics changes from overdamped to un-

derdamped (inertial) dynamics. We also show results for energy minimization dynamics that correspond to $\Gamma \rightarrow \infty$. Vibrational modes with frequency $\omega > \Gamma$ are underdamped, and it is useful to compare ω to the root mean squared or Einstein frequency $\omega_E \equiv \sqrt{\langle \omega^2 \rangle} = 17\tau^{-1}$.

We focus on the steady state achieved after plastic rearrangements have erased memory of the initial state ($\epsilon > 7\%$). While the system is trapped in a local energy minimum, work done by the applied strain leads to a nearly linear rise in potential energy and shear stress σ_s . When the minimum becomes unstable, there is a rapid avalanche of activity that leads to a sharp drop by E in energy and by $\Delta\sigma_s$ in shear stress. In the overdamped limit, the system is trapped in the next local energy minimum. When damping is reduced, inertia can carry particles over subsequent energy barriers to reach lower energy states. One dramatic consequence is that the mean energy sampled by systems decreases by 30% as Γ decreases. Indeed, there is almost no overlap between the ranges of energy sampled for the three damping rates studied in detail below, $\Gamma\tau = 1, 0.1$ and 0.001 .

To quantify the distributions of energy drops, we define the event rate $R(E, L)$ as the number of events of energy E per unit energy and unit strain in a system of size L^d with dimension $d = 2$. A sum rule relates $R(E, L)$ to the distribution of stress drops if $\Delta\sigma_s$ is much smaller than the mean shear stress $\langle \sigma_s \rangle$ and the shear modulus μ is nearly constant [19]. The energy dissipated by avalanches comes from work on the system during stress increases. We introduce an elastic energy $S \equiv \Delta\sigma_s L^d \langle \sigma_s \rangle / 4\mu$ associated with a given stress change, where $\langle \sigma_s \rangle / 4\mu \approx 0.02$ for all Γ and is independent of L . In steady state, the sum over stress drops equals the sum over stress increases and energy conservation requires: $\int dE E R(E, L) = \int dS S R(S, L) = L^d \langle \sigma_s \rangle$, where the last quantity is the total work per unit strain. Given the scaling exponents obtained below, both integrals are dominated by large events and thus $R(E, L)$ and $R(S, L)$ must exhibit the same scaling for large avalanches. Direct comparison of E and S for individual events shows that they are not proportional for small events and we consider the scaling of both distributions below.

Avalanche distributions are analyzed with finite-size scaling methods [20] that assume the maximum size of events $\sim L^\alpha$ is limited only by the system size L . The equations are developed for E but also apply to S . The distribution is assumed to obey the finite-size scaling ansatz:

$$R(E, L) = L^\beta g(E/L^\alpha) \quad , \quad (1)$$

where g is an unknown scaling function. Using the sum rule in the previous paragraph, one finds a scaling relation $\beta + 2\alpha = d = 2$ as long as the integral of $xg(x)$ is well defined.

Equation 1 produces power law scaling for $E \ll L^\alpha$ if $g(x) \propto x^{-\tau}$ for $x \ll 1$. One finds $R(E, L) \propto L^\gamma E^{-\tau}$ with $\gamma \equiv \beta + \alpha\tau$. One might expect that the probability of a small event in a given region would be independent of system size. This would imply a hyperscaling relation $\gamma \equiv \beta + \alpha\tau = d$ and $\tau = 2$, given the above relation $\beta + 2\alpha = d$. As shown below, $\tau < 2$ and the number of small events rises much less rapidly than L^d in our simulations ($\gamma < d$). Thus as L increases large events suppress small events either by changing the local configurations so small events are less likely to occur, or by increasing the probability that the same local configuration will produce a large avalanche. To our knowledge, the same behavior is not observed in other systems that display power law avalanche distributions. For example, the probability of small events is proportional to the size of the interface in models of fluid invasion or domain wall motion [7, 8].

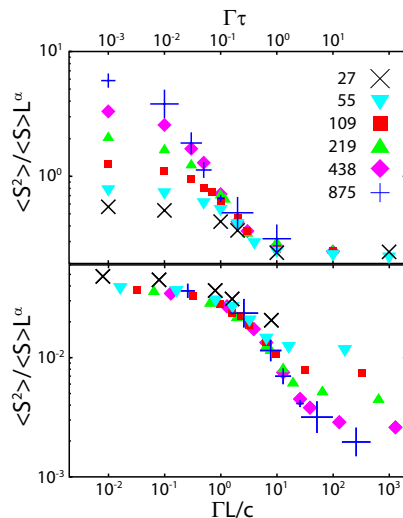


FIG. 1: Size of stress drops normalized by L^α plotted against (a) $\Gamma\tau$ with $\alpha = 0.85$ and (b) $\Gamma L/c$ with $\alpha = 1.6$. Statistical errors are smaller than the symbols for the indicated L/a .

We first show how Γ influences the scaling of large events with L . The mean size $\langle S \rangle$ is not well-defined because of the diverging number of small events for $\tau \geq 1$. Instead we show the ratio $\langle S^2 \rangle / \langle S \rangle L^\alpha$, which gives similar event sizes and scaling as other moment ratios. As shown in Fig. 1(a), $\alpha = 0.85$ collapses results for all L onto a universal curve for $\Gamma\tau > 0.1$. Results for $\Gamma\tau \geq 1$ and energy minimization are statistically indistinguishable. As $\Gamma\tau$ decreases from 1 to 0.1, the mean avalanche size increases in the same way for all L . Since $\omega_E\tau = 17$, systems remain in the overdamped universality class even when almost all vibrational modes are underdamped. The key factor is not whether modes are overdamped but whether inertia can carry the system over the next energy barrier in the energy landscape. A small Γ can trap the system in the nearest minimum if the difference

in successive energy barriers is small and/or the path in phase space to the next barrier is complicated.

As $\Gamma\tau$ decreases below 0.1 in Fig. 1(a), results for different L separate. As shown in Fig. 1(b), results in this underdamped limit can be collapsed using $\alpha = 1.6$ and scaling Γ by the time L/c for sound propagation across the system at shear velocity $c = 3.4a/\tau$. Data for $L > 27a$ follow a common scaling curve until $\Gamma\tau$ exceeds 0.1, and the critical behavior changes to overdamped. For $\Gamma L/c \ll 1$, all sound waves in the system are underdamped and all results tend to the same value of $\langle S^2 \rangle / \langle S \rangle L^\alpha$. As $\Gamma L/c$ increases past unity, the longest wavelength modes begin to be overdamped. The scaling exponent does not change, but $\langle S^2 \rangle / \langle S \rangle L^\alpha$ decreases. This is consistent with avalanches being cutoff by the wavelength of the largest underdamped mode rather than the system size. For the damping used here, this wavelength scales like $1/\Gamma$ and any finite damping takes the system away from the underdamped critical point. However, long wavelength modes are always underdamped as $L \rightarrow 0$ in disordered solids because dissipation mechanisms must be Galilean-invariant and only damp relative velocities [21]. Weakly damped simulations with two different Galilean-invariant thermostats [18, 22] gave statistically identical results to those shown in Figs. 1-3 for $\Gamma L/c < 0.1$.

We now examine the avalanche scaling in more detail in the overdamped ($\Gamma\tau = 1$) and underdamped ($\Gamma\tau = 0.001$) limits and at the crossover between them ($\Gamma\tau = 0.1$). Figure 2 shows $R(S, L)/L^\gamma$ vs. S in an overdamped system (lower curves). Power law scaling is observed from $S \sim 0.2u_0$ to a cutoff that increases with L . Data in this scaling regime are collapsed with $\gamma = 1.3 \pm 0.1$. As noted above, $\gamma < d$ implies that the number of events per unit area at a given S is strongly suppressed as L increases.

Figure 3 shows finite-size scaling collapses of overdamped data for both E and S (middle curves). The scaling factor in S was chosen so that the two quantities are comparable for large events, but the correlation between E and S breaks down below $0.2u_0$. Both quantities are well described by common scaling exponents Table (I) from $0.2u_0$ up to the largest event sizes.

At lower energies, $R(S, L)$ saturates while $R(E, L)$ follows a different power law that changes slightly with L . It is easy to confuse this power law with critical scaling if one only has results for $R(E, L)$ at small L . The noncritical power law dominates $R(E, L)$ for the smaller system sizes $L < 109a$ used in previous studies. This explains deviations in the reported values of α [13, 19] and why some papers concluded there was no critical behavior [23, 24]. Dahmen has recently suggested that τ has a mean-field value of 1.5 for all d in overdamped systems [25]. Our result of 1.2 is lower, but substantially higher than the values of $\tau < 1$ that would be inferred from the noncritical power law region in $R(E, L)$ [13, 23].

Figure 2 also shows $R(S, L)/L^\gamma$ for underdamped sys-

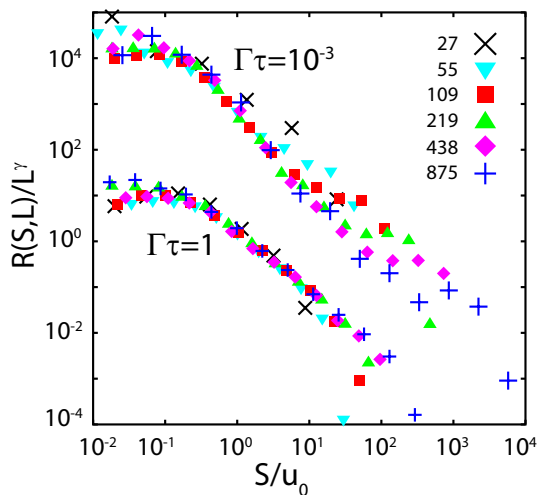


FIG. 2: Scaling of $R(S, L)$ with S for overdamped $\Gamma = 1$ systems with $\gamma = 1.3$ (lower curves) and underdamped $\Gamma = 0.001$ systems with $\gamma = 1.2$ (upper curves). Underdamped curves are multiplied by 100 to prevent overlap, symbols indicate L/a and symbol size is larger than statistical errors.

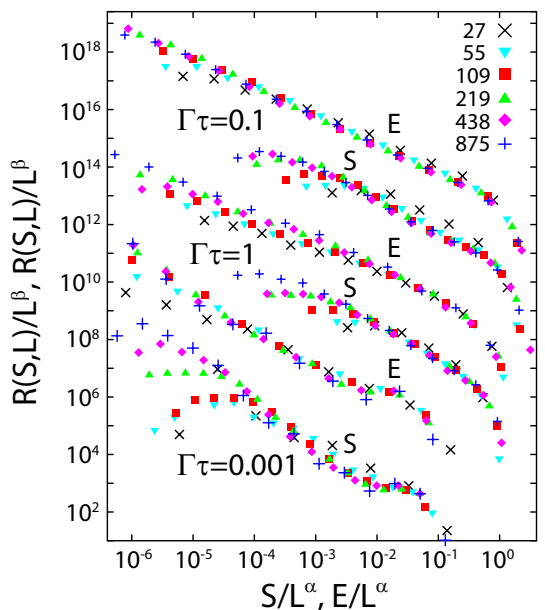


FIG. 3: (a) Finite-size scaling collapse of $R(S, L)$ and $R(E, L)$ for overdamped systems ($\Gamma\tau = 1$), underdamped systems ($\Gamma\tau = 0.001$) and critically damped systems ($\Gamma\tau = 0.1$) using the exponents in Table I. Statistical errors are smaller than the symbols and successive curves are shifted up by 2 or 3 decades to prevent overlap.

tems (upper curves). As expected, inertia leads to much larger avalanches. Results in the scaling regime for $S > 0.2u_0$ collapse with $\gamma = 1.2$. The distributions all show a power law decay followed by a plateau that moves to larger S as L increases. While this is different from the sharp cutoff in the underdamped case, the form of the scaling function $g(x)$ in Eq. 1 need not be simple.

Γ	τ	α	β	γ
1.0	1.2 ± 0.05	0.85 ± 0.05	0.3 ± 0.05	1.3 ± 0.05
0.1	1.0 ± 0.05	0.85 ± 0.05	0.4 ± 0.05	1.2 ± 0.05
0.001	1.5 ± 0.1	1.6 ± 0.1	-1.2 ± 0.1	1.2 ± 0.1

TABLE I: Scaling exponents determined for overdamped ($\Gamma = 1$) and underdamped ($\Gamma = 0.001$) limits and at the crossover between them $\Gamma = 0.1$. Quoted values satisfy the scaling relations $\beta + 2\alpha = d$ and $\gamma = \beta + \alpha\tau$ and errorbars are estimated from the quality of finite-size scaling collapses for E and S using other Γ and moments.

Figure 3 shows finite-size scaling collapses for S and E with the same scaling exponents (lower curves). In both cases, results for large events from different L collapse onto a universal curve. There is a plateau over a fixed range of a little under a decade followed by a very rapid decrease.

These results clearly imply that inertia does not destroy critical behavior, but does lead to a different universality class. Results for Galilean invariant thermostats with weak damping show the same scaling behavior. While our system lacks the complexity found in earthquake faults, it is interesting to note that τ is close to the value of ~ 1.6 for the Gutenberg-Richter law [26]. In addition, the distribution of earthquakes for a given fault system typically has an excess of large events that is similar to the plateau seen in Fig. 3 [26].

The final example we consider is the intermediate case of $\Gamma\tau = 0.1$ that seems to represent a crossover between overdamped and underdamped scaling in Fig. 1. Figure 3 shows a finite-size scaling collapse of $R(E, L)$ and $R(S, L)$ (top curves). The results follow a power law with $\tau = 1$ over 6 decades or more. Similar scaling was found for intermediate damping with Galilean invariant thermostats, for different interaction potentials, for simple shear, and in preliminary studies of 3D systems. This suggests that $\Gamma\tau = 0.1$ represents a multicritical point separating regions that flow to underdamped and overdamped fixed points.

In conclusion, introducing inertia does not destroy critical scaling of avalanches in quasistatic shear of disordered solids. Systems continue to be in the overdamped universality class even when most vibrational modes are underdamped. Only a small amount of damping is needed to prevent inertia from carrying systems over sequential energy barriers, implying that the difference between energy barriers is small or the path between them complex. Below a critical damping rate a new universality class corresponding to the underdamped limit is identified. The exponent describing avalanches is close to the Gutenberg-Richter law and the finite-size scaling function has an unusual form with a plateau before the cutoff at large events. Different scaling exponents are observed at the critical damping rate, indicating that it is a multicritical point.

The scaling exponents in all three regimes (Table I) satisfy the scaling relations $\beta + 2\alpha = d$ and $\gamma = \beta + \alpha\tau$. The hyperscaling relation $\gamma = d$ is violated in all cases. The number of avalanches at a given energy rises less rapidly than system size ($\gamma < d$), indicating that small events are suppressed by the larger events in bigger systems. Exponents obtained from finite-size scaling of the distribution of energy and stress drops are consistent. However, there is a long power law tail in $R(E, L)$ at small E with a size dependent exponent and system-size independent cutoff. This tail appears to have dominated previous determinations of α [13, 19] and τ [23, 27] using smaller systems.

We thank Karin Dahmen for useful discussions. This work was supported by the National Science Foundation (NSF) under grants DMR-10046442, CMMI-0923018, and OCI-108849.

-
- [1] J. Sethna, K. Dahmen, and C. Myers, *Nature* **410**, 242 (2001), ISSN 0028-0836, 10.1038/35065675.
 - [2] B. Gutenberg and C. F. Richter, *Bulletin of the Seismological Society of America* **34**, 185 (1944).
 - [3] P. A. Houle and J. P. Sethna, *Phys. Rev. E* **54**, 278 (1996).
 - [4] E. Vives, I. Ràfols, L. Mañosa, J. Ortín, and A. Planes, *Phys. Rev. B* **52**, 12644 (1995).
 - [5] S. Brinckmann, J.-Y. Kim, and J. R. Greer, *Phys. Rev. Lett.* **100**, 155502 (2008).
 - [6] M. C. Miguel, A. Vespignani, S. Zapperi, J. Weiss, and J.-R. Grasso, *Nature* **410**, 667 (2001), ISSN 0028-0836, 10.1038/35070524.
 - [7] N. Martys, M. O. Robbins, and M. Cieplak, *Phys. Rev. B* **44**, 12294 (1991).
 - [8] H. Ji and M. O. Robbins, *Phys. Rev. B* **46**, 14519 (1992).
 - [9] C. P. Prado and Z. Olami, *Phys. Rev. A* **45**, 665 (1992).
 - [10] G. A. Held, D. H. Solina, H. Solina, D. T. Keane, W. J. Haag, P. M. Horn, and G. Grinstein, *Phys. Rev. Lett.* **65**, 1120 (1990).
 - [11] H. M. Jaeger, C.-h. Liu, and S. R. Nagel, *Phys. Rev. Lett.* **62**, 40 (1989).
 - [12] J. M. Carlson and J. S. Langer, *Phys. Rev. Lett.* **62**, 2632 (1989).
 - [13] C. Maloney and A. Lemaître, *Phys. Rev. Lett.* **93**, 016001 (2004).
 - [14] N. P. Bailey, J. Schiøtz, A. Lemaître, and K. W. Jacobsen, *Phys. Rev. Lett.* **98**, 095501 (2007).
 - [15] H. G. E. Hentschel, S. Karmakar, E. Lerner, and I. Procaccia, *Phys. Rev. Lett.* **104**, 025501 (2010).
 - [16] A. Lemaître and C. Caroli, *Phys. Rev. E* **76**, 036104 (2007).
 - [17] H. G. E. Hentschel, S. Karmakar, E. Lerner, and I. Procaccia, *Phys. Rev. Lett.* **104**, 025501 (2010).
 - [18] C. E. Maloney and M. O. Robbins, *Journal of Physics: Condensed Matter* **20**, 244128 (2008).
 - [19] E. Lerner and I. Procaccia, *Phys. Rev. E* **79**, 066109 (2009).
 - [20] V. Privman, *Finite size scaling and numerical simula-*

- tion of statistical systems* (World Scientific, 1990), ISBN 9789810201081.
- [21] L. Landau, E. Lifshitz, A. Kosevich, and L. Pitaevskiĭ, *Theory of Elasticity*, Theoretical Physics (Butterworth-Heinemann, 1986), ISBN 9780750626330.
- [22] P. J. Hoogerbrugge and J. M. V. A. Koelman, *EPL (Europhysics Letters)* **19**, 155 (1992).
- [23] S. Tewari, D. Schiemann, D. J. Durian, C. M. Knobler, S. A. Langer, and A. J. Liu, *Phys. Rev. E* **60**, 4385 (1999).
- [24] T. Hatano, *Phys. Rev. E* **79**, 050301 (2009).
- [25] K. Dahmen, Y. Ben-Zion, and J. T. Uhl, *Nature Physics* **7**, 554 (2011), ISSN 1745-2473.
- [26] C. Scholz, *The mechanics of earthquakes and faulting* (Cambridge University Press, 2002), ISBN 9780521655408.
- [27] C. E. Maloney and A. Lemaître, *Phys. Rev. E* **74**, 016118 (2006).